Nonvolatile photorefractive spectral holography

Kazutaka Oba, Pang-Chen Sun, and Yeshaiahu Fainman

Department of Electrical and Computer Engineering, University of California, San Diego, La Jolla, California 92093-0407

Received February 12, 1998

We demonstrate nonvolatile storage of femtosecond pulses in a photorefractive $LiNbO_3$ crystal with recording and readout of spectral holograms at wavelengths of 460 and 920 nm, respectively. No degradation was observed after 24 h of continuous readout. We also show that we can realize the time-lens effect with our system by appropriately setting the ratio of the recording and the reconstruction wavelengths and the spectral resolution of the recording and the reconstruction processes. © 1998 Optical Society of America

OCIS codes: 090.0090, 190.5330.

Three-dimensional (3-D) optical memories, by extending storage into the third dimension, permit higher capacities and bandwidth. Various physical mechanisms for 3-D storage have been explored, including volume holography in photorefractive materials,[1–5] two-photon recording,[6] spectral hole burning,[7] and photon echo.[8] 3-D memory systems based on volume holographic storage have been investigated with respect to optimization of materials, devices, data structures, and systems for ultrahigh storage density with millisecond access times and terabits-per-second aggregate transfer rates. With the exception of spectral hole burning or photon-echo optical storage, most of the 3-D storage systems under development achieve a high aggregate bandwidth by storing and accessing pages of bits as opposed to a single bit as in a conventional CD-ROM. During readout, an appropriate code is set for the reference beam that reconstructs the corresponding page of information at the output of the memory system. Although the page-oriented approach may be useful for local data access, processing, and communication of images and image-format data, it is unlikely that page-oriented optical memories can be easily integrated with distributed-information systems that utilize ultrahigh-bandwidth optical network systems. Parallel-to-serial format-conversion input–output devices[9] will need to be developed for integration of such page-oriented storage systems with communication network systems. These conversion devices must at least preserve the aggregate bandwidth of the storage system or even multiplex a few storage systems to meet and utilize the ultrahigh bandwidths of evolving optical communication network systems. In view of this requirement we anticipate that many applications will benefit from an optical holographic memory, which stores and retrieves information in a format that is suitable for direct interface with and transmission through an optical fiber network, thereby providing optimal performance in terms of hardware complexity, memory and network capacity, bandwidth, and latency. With such an approach the spatial image information is converted to a time-domain sequence and stored as a spectral hologram. The information retrieved from the memory is output in a time-sequence format suitable for direct transmission over optical fiber networks at rates exceeding 1 Tbit/s. At the network receiver node, the time-sequence data can be demultiplexed by conversion of the time-sequence back to parallel spatial channels for electronic detection, processing, and display. In this Letter we demonstrate nonvolatile photorefractive storage of femtosecond pulses by use of a spectral holographic technique in which the information retrieval speed of the storage system can match the full bandwidth of an optical fiber network and show the potential for a time-domain-transparent optical storage system.

Spectral holography[10] can store and reconstruct a train of ultrashort pulse signals by holographic recording of spatially dispersed optical frequency components. The experimental setup consists of a 4F system with gratings located at the front focal plane of the first Fourier transform lens and at the back focal plane of the second Fourier transform lens. The storage material is placed in the Fourier transform plane of this 4F system, i.e., the back focal plane of the first Fourier transform lens. Previous research on direct time-domain recording[11] showed that the number of pulses that can be stored in a hologram is determined by the size of the crystal. In contrast, the number of pulses that can be stored in a hologram in a spectral holographic system is determined by its time aperture.[9]

We use a photorefractive crystal as the real-time storage material to implement the spectral holographic write–read process. One of the issues associated with photorefractive holographic memory is volatility. That is, if the same wavelength of light is used for recording as well as for reconstruction in a photorefractive process, then the reconstruction process could also erase the recorded hologram. We addressed this issue by reconstructing the recorded information by use of radiation at a wavelength for which the sensitivity of the photorefractive material is essentially zero, provided that we satisfy the Bragg-matching condition at the reconstruction wavelength to obtain efficient readout. Several elaborate solutions to the Bragg-matching condition in page-oriented holographic memory systems in which dual-wavelength recording and reconstruction were employed were proposed.[12] In our proposed spectral holography scheme, however, dual-wavelength recording and

0146-9592/98/120915-03$15.00/0

reconstruction do not require any special arrangement to satisfy the Bragg-matching condition. One can satisfy this condition over the entire spatial frequency range by changing the incident angle appropriately, because holograms recorded by this method have a quasi-one-dimensional data format, and it is possible to choose the direction of the spatial carrier to be orthogonal to the direction of the wavelength spread (i.e., to direction encode the information).

The experimental setup is schematically shown in Fig. 1. We use a mode-locked Ti:sapphire laser (Mira Model 900-F; Coherent) that produced 200-fs pulses with center wavelength 920 nm and a repetition rate of 77 MHz. The infrared radiation (920 nm) is divided into two beams, one of which is kept for the hologram reconstruction process while the other one is frequency doubled by a second-harmonic generator that produces pulses at a wavelength of 460 nm for hologram recording. The radiation at 460 nm is split into two beams, one used as a reference beam and the other transmitted through a pulse shaper to produce an object-beam pulse sequence. The pulse sequence is tailored by means of spectral domain filtering of an incident transform-limited pulse introduced into the pulse shaper.[13] The shape of the pulse sequence is proportional to the time-domain convolution between the transform-limited input pulse and the Fourier transform of the spectral filter in the pulse shaper. For example, if we use a grating as the spectral filter of the pulse shaper, the shape of the output pulse will consist of a time sequence of an equally spaced train of pulses. We can calculate the time separation Δt_w between the adjacent pulses during the hologram writing step to be

$$\Delta t_w = \frac{2\pi \alpha_w F_w}{\Delta x_w \omega_c}, \tag{1}$$

where F_w is the focal length of the Fourier transform lens in the pulse shaper, Δx_w is the grating period, ω_c is the angular frequency of the center wavelength of the pulse, and $\alpha_w = f_w \lambda_w$ (here f_w is the grating frequency and λ_w is the center wavelength). In our experiment we use a pulse-shaper lens with $F_w = 250$ mm and a Ronchi grating with $\Delta x_w = 100$ μm, producing a pulse sequence with time separation $\Delta t_w = 2.1$ ps (corresponding to a data transmission rate of 0.47 Tbits/s).

The object beam from the pulse shaper and the reference pulse are introduced into the spectral holographic storage system shown in Fig. 1(a). The two beams propagate parallel to each other but are separated vertically by 2.5 cm to introduce a spatial carrier for recording of the spectral hologram. The optical path-length difference between the reference and the object beams is adjusted by a delay line that is introduced into the path of the reference beam. Both beams diffract from the first reflection grating of 2400 lines/mm and then are spatially Fourier transformed by the first lens (focal length, 375 mm). The spectral decomposition wave components of both the signal pulse and the reference pulse are identically spread in the horizontal direction, whereas they merge and overlap in the vertical direction. The spectral components from each beam coincide, producing an interference pattern that can be recorded as a spectral hologram. A 1-mm-thick $LiNbO_3$ crystal is placed in the Fourier transform plane for recording of the spectral hologram. Typical recording times vary in an interval of 60–90 s. As the recording process takes a relatively long time, the stability of the system is crucial.

During the reconstruction process, a 920-nm wavelength readout pulse beam is introduced into the recording system by a dichroic beam splitter, which reflects radiation at 920 nm while transmitting radiation at 460 nm. The readout beam, after it is diffracted from a 600-line/mm reflection grating, is Fourier transformed by a lens with a focal length of 375 mm. To satisfy the Bragg-matching condition, we shift the readout beam vertically to achieve the best diffraction efficiency from the spectral hologram. In our experiment we set the scaling factor to 1 by choosing gratings with appropriate spatial frequencies. The reconstructed beam from the hologram is transmitted through the second Fourier transform lens and combined by the second reflection grating of 600 lines/mm. The reconstructed pulses are introduced into an autocorrelator (BX-514; Inrad) for detection and analysis.

Figure 2 shows the experimental results of the reconstructed pulse sequence that was stored in the spectral hologram. The reconstruction result shows that each of the reconstructed pulses has a pulse width of ~200 fs and that the pulse separation is 1.97 ps, consistent with the calculated pulse separation of 2.1 ps with the scaling factor of ~1. The diffraction efficiency was measured to be 7% and did not show any degradation for more than 24 h of continuous reconstruction. Second-order peaks appeared as a result of imperfections in the Ronchi grating that was used in our experiment.

For dual-wavelength spectral holography used in writing and reading of a hologram, the time separation of the readout pulse train can be larger or smaller than that of the input recorded pulse train. This phenomenon is similar to the effect of magnification in conventional spatial holography when different wavelengths are used during writing and reading of the hologram.

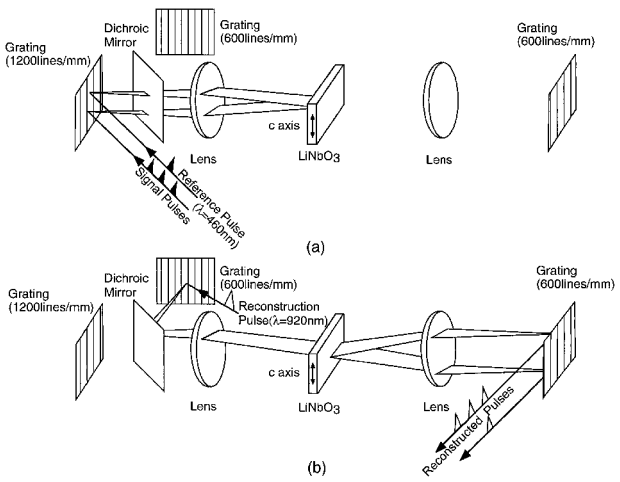

Fig. 1. Time-domain storage system using a spectral holographic recording system: (a) recording setup, (b) reconstruction setup.

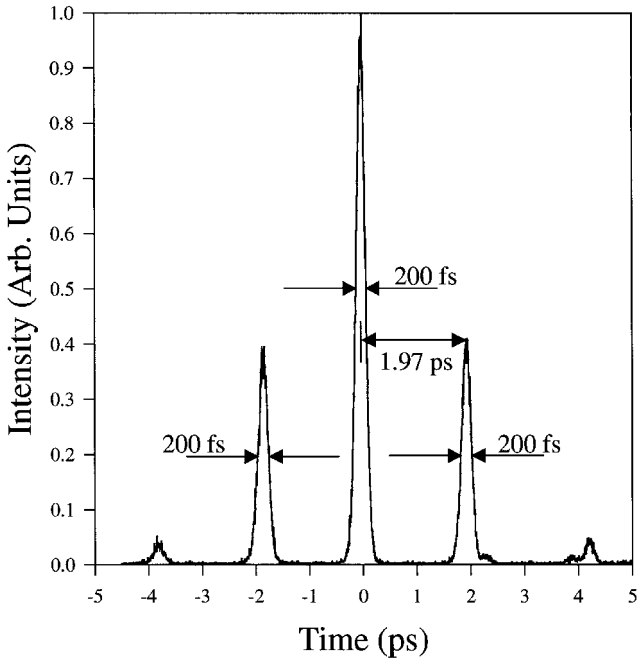

Fig. 2. Trace from an autocorrelator showing the reconstructed time sequence stored in a spectral hologram.

The reconstructed image can be magnified or demagnified, depending on the ratio of the writing and reading wavelengths. In contrast, the magnification in spectral holography is also affected by the spectral resolving power of the gratings used during the recording and reconstruction processes. To determine the time magnification in spectral holography, we need to find the time-scale change. Consider recording a signal consisting of a pair of short pulses separated in time by Δt_w. The separation of the reconstructed pulses, Δt_r, is given by

$$\Delta t_r = \frac{f_r \lambda_r^2}{f_w \lambda_w^2} \Delta t_w , \tag{2}$$

where λ_r and λ_w are the wavelengths and f_r and f_w are the spatial frequencies of the gratings used during the reconstruction and recording processes, respectively. The effect can be regarded as time imaging[14] if the recording and the reconstruction processes satisfy the time–bandwidth product matching condition

$$D_r f_r \frac{\Delta\Omega_r}{\omega_r} = D_w f_w \frac{\Delta\Omega_w}{\omega_w} , \tag{3}$$

where D_r and D_w are the pupil sizes of the optical field illuminating the reflecting gratings, ω_r and ω_w are the angular frequencies of the center wavelengths, and $\Delta\Omega_r$ and $\Delta\Omega_w$ are the pulse bandwidths of the reconstruction and the recording pulses, respectively. For example, it is possible to record a spectral hologram of nanosecond pulse signals and reconstruct them with subpicosecond-scale pulses, yielding nearly 1000-times magnification. For this application, a high-spectral-resolution device, such as a Fabry–Perot interferometer, is required for spectral decomposition of the nanosecond pulses.[15]

We have demonstrated nonvolatile photorefractive spectral holography for time-domain storage of femtosecond pulses. No degradation was observed after 24 h of readout. We also showed that the time-lens effect can be realized by our system when the wavelength and the spectral resolution of the recording and the reconstruction processes satisfy the time–bandwidth-product matching conditions. Our demonstration shows that this technique can support an all-optical transparent read and write data-storage system with readout speed matching the speed of optical fiber network systems.

To use this approach for optical mass storage, we need to investigate multiplexing methods for increased storage capacity. We are currently exploring the space-multiplexing method of our spectral holographic technique, because the reference and the signal pulses are focused into a small area, occupying an increasingly narrow width.

This study was supported in part by the Ballistic Missile Defense Organization, the U.S. Air Force Office of Scientific Research, and the National Science Foundation.

References

1. J. E. Ford, J. Ma, Y. Fainman, S. H. Lee, Y. Taketomi, D. Bize, and R. R. Neurgaonkar, J. Opt. Soc. Am. A **9,** 118 (1992).
2. Y. Fainman, Proc. SPIE **1150,** 120 (1989).
3. D. Brady and D. Psaltis, J. Opt. Soc. Am. **9,** 1167 (1992).
4. L. Hesselink and M. Bashaw, Opt. Quantum Electron. **25,** S611 (1993).
5. Y. Fainman, J. Ma, and S. H. Lee, Mater. Sci. Rep. **9,** 53 (1993).
6. J. Ford, S. Hunter, R. Piyaket, Y. Fainman, S. Esener, S. Dvornikov, and P. Rentzepis, Proc. SPIE **1153,** 604 (1993).
7. M. Mitsunaga, Opt. Quantum Electron. **24,** 1137 (1992).
8. X. Shen and R. Kachru, Appl. Opt. **32,** 5810 (1993).
9. P. C. Sun, Y. Mazurenko, and Y. Fainman, J. Opt. Soc. Am. A **14,** 1159 (1997).
10. Y. Mazurenko, Appl. Phys. B **50,** 101 (1990).
11. L. H. Acioli, M. Ulman, E. P. Ippen, J. G. Fujimoto, H. Kong, B. S. Chen, and M. Cronin-Golomb, Opt. Lett. **16,** 1984 (1991).
12. D. Psaltis, F. Mok, and H. Li, Opt. Lett. **19,** 210 (1994).
13. A. M. Weiner, D. E. Leaird, J. S. Patel, and J. R. Wullert, Opt. Lett. **15,** 326 (1990).
14. B. H. Kolner and M. Nazarathy, Opt. Lett. **14,** 630 (1989).
15. Y. Mazurenko, S. E. Putilin, V. V. Kuznetsov, and L. M. Lavrenov, Opt. Spectrosc. **71,** 223 (1991).